

Research article

Experimental investigation of improving the solar desalination system for domestic buildings: Iraq as a case of study

Layth Abed Hasnawi Al-Rubaye^{1,*}, Ahmed Al-Samari^{1,2}, Saad Theeyab Faris¹ and Saadoon Abdul Hafedh¹

¹ Department of Mechanical Engineering, College of Engineering, University of Diyala, Diyala, Iraq

² Mechanical and Aerospace Engineering Department (alumni, PhD), West Virginia University, 26505, USA

* **Correspondence:** Email: laythabed2014@gmail.com; Tel: +9647719223931.

Abstract: Iraq encounters climatic challenges that lead to severe rainfall shortages and compound the regional challenges that lead to reduced rates of supplying rivers. In this research, the proposed design helps obtain pure water from polluted or saline water at lower, more competitive costs that can supply nearly 80% of the Iraqi markets.

The system harvests 2 L/day of pure water by adding 5 liters of saline water, a 209% daily improvement. The system consists of 1.125 m² of double slope single basin solar still with a tilt angle of 30°, pipes, and measurement instrumentation.

Maximum inside temperature, humidity, valuable energy, and efficiency have 77 °C, 35%, 4.02 W/m², and 76%, respectively. System analysis results demonstrated that the average water condensation rate per square meter is about 0.4 L/hr. Finally, the rate of pure water harvesting from this desalination system, per square meter, is about 0.282 L/m² per day when the average intensity of solar radiation reaches 165 W/m². Two scenarios have been suggested for the experiment. The first scenario tests the system by limiting two water levels, the first at 0.75 cm and the second at 3 cm. The second scenario includes the same design with a black cloth set in the basin demonstrates the most promising data. A wet pad regularly cools down one side of the glass to increase the water vapor condensation and production quantity by 173% to enhancing water production significantly.

Keywords: solar energy; renewable energy; desalination water; domestic buildings; condensation

1. Introduction

Freshwater resources represent one of the most challenging environmental issues. Further, water is one of the most valuable resources for domestic buildings and developing modern architecture. In addition, it plays an essential role in sustainable development operations worldwide. Fresh water is necessary for the economy, food production, and human survival. The world is suffering from climatic changes that have reinforced the decline in rainfall and the scarcity of fresh water. The Arab region exists within the belt of waterless and drylands [1], suffering a significant shortage of freshwater.

The average per capita water availability is 10% of the world average. On the other hand, water demand is continuously growing due to the increasing rate of population growth [2]. The amount of water available in the Arab region is about 274 billion m³, distributed between surface water, internal rivers, or shared rivers from other countries [3]. However, available water from underground and desalinated sources is estimated at 62 billion m³. The annual utilization of renewable water within the Arab region reaches about 77% [4]. The world also shows sub-regional differences in the water supply. The Unified Arab Water report (UAW) for 2020 confirmed that Iraq is one of the Arab countries most vulnerable to water shortage disasters in recent years, as Iraq ranked 42nd within the "high risk" category [4]. Water desalination is one of the solutions to this crisis, but it's expensive. It's a problem for some Arab countries, as desalination technology could cause a financial crisis, if implemented [5]. Research and studies in this field have diversified and increased in recent years. With more than 20,000 plants worldwide, desalination enables countries to provide water security for future generations amid growing climate concerns [6]. This process produces freshwater by converting saline water or water reuse. But it needs energy to work, increasing the cost of production, and that increase in cost has prompted the world to find alternatives that reduce cost and increase production to provide reasonably priced water. Renewable energies and desalination systems are two different technologies; they can be used together by operating desalination systems using renewable energy sources [7].

In contrast, this technology is not without its drawbacks, as its use is associated with an increase in the value of the initial cost and the need to deal with large areas (about 250 m² per 1 m³ of pure water) [8]. Another challenge for such projects is economic analysis. Because it depends on variables that are not fixed globally, it also varies from one system to another. It needs to determine the financial recovery period and reduce the risks of project failure. The essential variables are the initial cost of the project, the benefit achieved, the annual distillation harvest, the maintenance cost for cleaning only, the project life cycle, the production price of pure water, the sale worth of purified water, the recover charge of the system, etc. [9]. The cost of producing pure water from these variables is calculated based on the initial investment and interest rate. The advantages are to help enhance drinking water in arid or semi-arid regions with abundant renewable energy sources and not having traditional energy supplies (such as electricity networks) for desalination [5]. Solar energy for desalination is a promising technology for supplying potable water. Desalination is not a new technology, so it is considered one of the oldest methods of water refinement known to humans. Iraq has more than 3000 hours a year of sunshine used for water heating [6]. This green energy helps to use solar collectors well and is acceptable. In the past five years, Iraq has tended to enhance the possibility of using solar energy. It has limited it to only two aspects: photovoltaic units to help produce electricity or solar collectors to output hot water. It's limited to small local projects for

homes and a few government institutions. However, this energy is not used to account for desalination [9].

This work concentrates on building a new proposed design for the solar desalination unit by using a simplified and practical method to produce, drink, and cook water from salty and unclean water. Many experiments were conducted to obtain pure water from various sources (seas, wells, and water swamps), all of which required more energy. Recent investigations have reinforced the possibility of reducing energy costs for obtaining pure water by integrating solar energy into the desalination system. Although it is technically complex due to the irregularity of solar radiation throughout the year, the future will depend only on renewable energies such as solar energy because they will not emit harmful gases [10], which will improve the environment and encourage regular rainfall. Many experiments and research are dealing with the issue of water desalination worldwide. Which have proven the efficacy of solar collectors in desalination, such as:

Abdel-Rehim, et al. [11] conducted an empirical study that reinforced the theoretical aspect of the solar water desalination system in Cairo, Egypt. By using a conventional desalination unit modified to include a concentric solar parabolic trough and a simple heat exchanger (copper serpentine) insulated to take advantage of the heat during the day and night. The oil was used as a heating fluid in the heat exchanger. During the day, seawater is heated directly by solar radiation and heat storage for nocturnal production. The results showed that freshwater productivity increased by an average of 18% due to the modification. In contrast, the current work is characterized by the development of the traditional system for desalination water by using double slope single basin solar still to harvest the most significant possible amount of solar radiation. And to avoid the problems and obstacles of heat storage.

Yuan et al. [12] researchers worked on designing an experiment for a water desalination system to produce 1000 L/day in China. The system consists of 100 m² of solar air heater field, 12 m² of solar water collector, dehumidifying unit, a pre-treatment and post-treatment system and other sub-systems. The researchers examined the system's performance and performed several water production tests on emblematic days. The results showed a harvest of 1200 L/day of fresh water when the average intensity of solar radiation reached 550 W/m².

This work is accordance with the recent experiments that relied on low-cost, simple materials. Comparing the average sun heat in Iraq, which reaches 630 W/m², with the amount of production, it is good compared to their work, the area, and advanced technology.

To determine the limitations and determinants of the proposed mechanism, particularly the extent to which it is economically feasible. Several researchers, including El-Bialy et al. [13], worked to deliver a comprehensive cost analysis for the various configurations of solar water desalination devices (passive and active). Depending on the calculation of cost analysis factors, by entering the manufacturing charge (P) and the yearly return ($M = \text{average daily productivity} \times 260 \text{ days}$) for ten years using the Excel program. The results showed that the economic feasibility of these collectors is competitive and acceptable related to the price per liter in both the Egyptian and Saudi markets.

In turn, the economic extent of the proposed system was calculated, which showed that the annual return amounted to 520 L/year at a manufacturing cost of \$200, for 0.4 \$/L, with an improvement rate of up to 85% per year, which achieved a feasible and effective economic return. This makes it the first study in Iraq to calculate the economic feasibility of using this type of water desalination device.

The interest in providing fresh water has increased due to the population explosion and finding alternative production methods at the lowest cost. There has been a tendency to use solar energy for desalination purposes in various ways, including traditional, passive, and active systems. Abuelnuor et al. [14] worked on the progress of a pilot study to address the problem of low daily productivity of a fixed water desalination system, a solar panel solar collector and paraffin wax as a phase change material (PCM) solar powered to produce pure water. The researchers concluded that the cumulative productivity of conventional solar distillation could be improved by between 85% for the passive system and 121% for the active system. The results confirmed that the combination of the passive and active systems had the highest performance, reaching 164%. Based on this, the improvement rate in the currently proposed system has reached 209% for desalinating brackish water.

Hanane et al. [15] worked on an experiment to study the inside bounds of a double-slope solar panel for brackish water desalination. Experiments were conducted in different atmospheric conditions, which proved that the pure water production rate improves by decreasing the difference between the temperature of the basin and the glass. The outputs are also affected by wind and climatic changes that reduce solar radiation. The results showed that the average production of distilled water was 4 L/m²/day. That is evident in practice in the current experience.

Choong et al. [16] investigated pyramid and single-basin solar under the same operational conditions in Basra city in Iraq. It was determined that the productivity of the pyramid solar still was optimal at 7.36 L/day. While Nafey et al. [17] are working on the possibility of using simple solar desalination in the northern areas of Iraq. By using different operational variables that affect solar performance, like water thickness and wind speed. This study shows these variables affected the salinity of the water leading to a reduction in productivity. A recent study in Iraq's desert areas by Jamil et al. [18]. To observe the effect of external cooling on the amount of water yield in this study, researchers used a new pyramid solar design with a 32.5° glass slope angle and 3 cm water level in the basin. The experimental outcomes observed that freshwater yield increased by a significant 370% when using external cooling fan. To speed up the heat time of the water in the basin, Omara et al. [19] conducted an experiment using a heating coil connected under the basin. It was powered by a PV cell and had distillation of up to 1089%.

Another experiment performed in Iraq by Tripathi et al. [20] built a hybrid system using solar distillation coupled with the solar pond technique as a renewable energy method in Iraq for 50 days. These tests showed a maximum temperature of (62–64) °C with an efficiency of 10%.

Also, AlKtranea et al. [21] Organizers of the work highlight the importance of using the Fresnel lens technology to enhance conventional solar still (CSS) productivity. Under the climate conditions of Basra city, Iraq. The experimental results showed better performance, about 68.6% at 1 cm depth and 59.3% at 2 cm depth. Table 1 shows the improvement in this study and previous studies by comparing the efficiency of the equipment and the differences between the results.

Table 1. The amount of improvement in the types of solar collectors in terms of absorption area, normal regular productivity and sunshine hours in Iraq.

Ref.	Absorbing area m ²	Average daily productivity l/day	Amount of improvement
Choong et al. [16]	1.5	7.36	145%
Nafey et al. [17]	3	3.25	125%
Jamil et al. [18]	2	1.75	220%
Omara et al. [19]	1.25	1.7	370%
Tripathi et al. [20]	1	2.5	160%
AlKtraneea et.al. [21]	2	80 to 215	285%

1.1. Novelty of the proposed work

Iraq is one country that needs to use renewable energy to reduce greenhouse emissions. The novelty of the proposed work is designed to reduce energy consumption for water desalination, which permits a decrease in increasing temperatures and improved rainfall. In addition to helping provide good sources of drinking water and daily use for remote areas, villages, and rural areas. This project represents the first step to studying the possibility of using single basin couple slope- solar stills in the middle of Iraq for desalination.

With the goal of developing this project in the future to fit with commercial production, this paper conducted a detailed economic analysis of the daily and annual production costs and compared them to the water production in the local markets. Also, the solar collector has been tested in practice, and its production is specific and not at the level of the production station.

2. Methodology

Turkey and Iran, neighboring Iraq, built several dams and many headwaters for Euphrates and Tigris rivers [17–19]. That caused a reduction in Iraq's water share and the wave of desertification and drought. Using solar energy for purifying water for human using is the cheapest approach.

In contrast, the effectiveness and production rate are relatively low in comparison to the other methods. Therefore, it is important to try increasing the effectiveness of the solar purification systems by modifying the design and method of pure water collections. Additionally, another goal is to ensure the design enables local inhabitants the materials and methods to construct this water purification technology on their own.

2.1. Solar stills system

The sun energy collector is an instrument that captures heat of solar energy and changes it is valuable thermal energy [21]. Renewable energy approach is active in transferring heat to evaporate water and enabling the fresh water harvesting. Solar energy for using heat production dates from antiquity. Further, this method is using to pass more heat and getting more pure water. The direct lunar warming methods utilize natural resources such as heat transfer by convection or radiation, thermosiphon flow, and thermal properties of materials to collect and transfer heat.

Iraq has solidarity ranging from 1800 kWh/m²/year to 2390 kWh/m²/year of direct average radiation [21], which places the country in an up-and-coming status, and at the forefront of countries

that produce electricity using solar energy [22]. Solar systems simulate the natural cycle of water. These systems benefit from the sun direct light and heat to the collector to evaporate the water inside the space. Then the condensation takes place on the glass cover and is collected as drinkable water. There are different significant designs of solar stills that several researchers have used. They are categorized into two systems: passive and active solar stills [23–25].

Many researchers are concentrated on the factors affecting still productivity using experimental techniques. This experience is only a supplement to their work and trying to find a simple design that deals seriously with the weather conditions in Iraq, especially in central Iraq, Diyala province. Figure 1 shows the considered solar still.

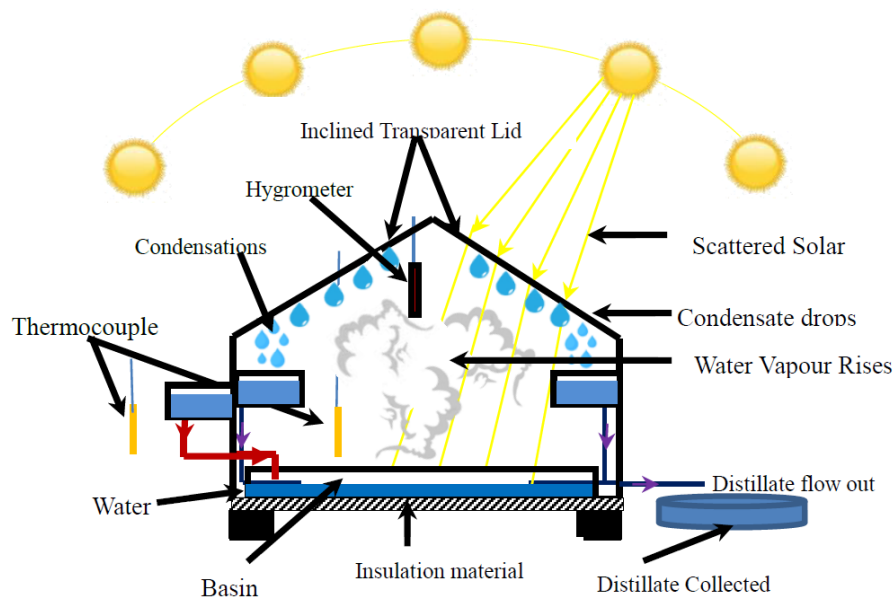


Figure 1. Solar still water proposed model design.

The solar energy is transferring by radiation to the purifying system and then heating the black pad then the impure water receiving heat by convection which make it boiling and evaporated. Therefore, the water vapor condenses on the inside glass surface because it cooler than saturation temperature [24].

2.2. Mathematical model of solar still

Renewable energy applications such as panels, collectors, and solar stills are not built horizontally but inclined to enhance the heat that entered the desalination system and decrease losses by reflection, there is a necessity to convert these data to radiation on tilted surfaces. The geometric factor R_b , which represents the ratio of ray radiation on the sloped surface to that on a horizontal surface at any time, can be deliberate as follows [25]:

$$R_b = \frac{RT}{R_n} = \frac{R_n \cos \theta}{R_n \cos \theta_z} = \frac{\cos \theta}{\cos \theta_z} \quad (1)$$

Therefore, the RT represents the sun radiation on a inclined surface. Moreover, the R_n is solar

heat transfer on a surface upright to the direction of spread. Finally, θ is the angle of the occurrence on a sloped exterior obtained from [10,11]:

$$\cos(\theta) = \sin(\delta) \sin(\phi) \cos(\beta) \sin(\delta) \cos(\phi) \sin(\beta) \cos(\gamma) \cos(\delta) \cos(\phi) \cos(\beta) \cos(\omega) + \cos(\delta) \sin(\phi) \sin(\beta) \cos(\gamma) \cos(\omega) + \cos(\delta) \sin(\beta) \sin(\gamma) \sin(\omega) \quad (2)$$

The equation for energy conservation through glass that cover the system is governed by [13]:

$$m_c C_c \frac{dT_c}{dt} = A_c (1 - p_c) \alpha_c I + q_{r,w-c} + q_{ev,w-c} + q_{c,w-c} - q_{r,c-a} - q_{c-c} - a \quad (3)$$

m_c , C_c and α_c are represent the bulk, explicit heat and absorptivity of the transparent, respectively.

Figure 2 explains the mechanism of heat transferring and entering the purification system, then the system base absorbing it. Then the heat is transferring by convection to evaporate the saline water.

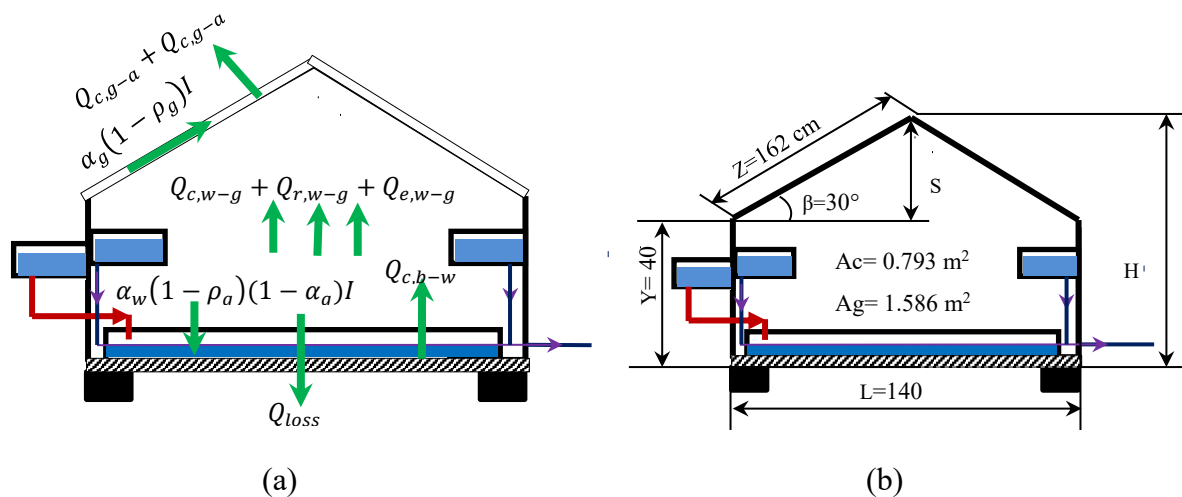


Figure 2. (a) Heat transfer process in solar still, (b) Dimensions and measurements.

The heat energy that lost by convection could expressed by the following equations. [13,14]:

$$q_{c,c-a} = (6.15V_{wind}^{0.8})A_c(T_c - T_{amb}) \text{ for } V_{wind} < 5 \text{ m/s} \quad (4)$$

$$q_{c,c-a} = (2.8 + 3V_{wind})A_c(T_c - T_{amb}) \text{ for } V_{wind} < 5 \text{ m/s} \quad (5)$$

Since the sky could be supposed to be a black body, then the following relation can present the infrared heat that exchanging between the glass and the sky [20–22]:

$$q_{r,c-a} = A_c \varepsilon_c \sigma \left[(T_{sky} + 273)^2 (T_c + 273)^2 \right] (T_c - T_{sky} + 546) (T_{sky} - T_c) \quad (6)$$

The atmosphere hotness is connected to the ambient temperature, as shown below [16–18]:

$$T_{sky} = 0.0522 \cdot T_{amb}^{1.5} \quad (7)$$

Using the assumption of the grey surfaces, the energy heat exchange between the glazing and the surface water is described as follows [19]:

$$q_{r,w-c} = [(T_c + 273)^2 (T_w + 273)^2] (T_c + T_w + 546) / (1/\epsilon_w + 1/\epsilon_c - 1) A_w (T_w - T_c) \quad (8)$$

The heat transfer by convection exchange between the glazing and the water surface can be estimated by the following equation [20,21]:

$$q_{c,w-c} = 0.884[(T_w - T_c) + \frac{(P_w - P_c)(T_w + 273.1)^5}{(268.9 \cdot 10^{-3}) - P_w}]^{0.33} A_w (T_w - T_c) \quad (9)$$

where P_w and P_c are, represent the fractional vapor pressures at the water apparent temperature and at the inside glazing surface and the following equation determines them [22,23]:

$$P_w = \exp(25.317 - [(5144/T_w) + 273.15]) \quad (10)$$

$$P_c = \exp(25.317 - [(5144/T_c) + 273.15]) \quad (11)$$

The boiling heat transfer interchange between the coating and the water surface can be determined as follows [24]:

$$q_{c,w-c} = (16.237 \cdot 10^{-3}) \frac{(P_w - P_g)}{(T_w - T_c)} \left[(T_w - T_c) + \frac{(P_w - P_c)(T_w)}{268900 - P_w} \right]^{0.33} A_w (T_w - T_c) \quad (12)$$

2.3. The base plate absorption

The energy balance for the absorber plate is given by [25–27]:

$$m_b C_b \frac{dT_b}{dt} = A_b (1 - \rho_c) (1 - \alpha_c) (1 - \alpha_w) \alpha_b I - q_{c,b-w} - q_{loss} \quad (13)$$

q_{loss} is a backward loss to the ambient temperature, and the following equation can determine it [28]:

$$q_{loss} = \left(\frac{L_b}{k_b} + \frac{L_i}{k_i} + \frac{1}{h_i} \right)^{-1} A_b (T_b - T_{amb}) \quad (14)$$

2.4. Thermal analysis

Solar heat rate represents the product of the effective area of the sun still and beam radiation in the following [28]:

$$Q_s = A_a \times I \quad (15)$$

where Q_s is solar energy (W), A_a the aperture is (m^2), and I is intensity solar radiation (W/m^2). The helpful heat collector (Q_u) can be calculated by the energy balance in the fluid volume by [29]:

$$Q_u = m' C_p (T_{out} - T_{in}) \quad (16)$$

where m' is the mass flow rate (kg/s), C_p is the specific heat capacity (J/Kg. K), T_{out} is the outlet temperature, and T_{in} is the inlet temperature ($^{\circ}C$). All the equations of radiation losses are described from the equation below [28]:

$$Q_{\text{loss}} = Q_{\text{conv}} + Q_{\text{rad}} \quad (17)$$

where Q_{conv} is convection heat transfer (W), Q_{rad} is a radiation heat transfer (W), and can be found from Eqs (18) and (19) [20–25].

$$Q_{\text{conv}} = A_r h_{\text{air}} (T_r - T_{\text{am}}) \quad (18)$$

where: A_r is receiver area (m^2), T_{am} represents ambient temperature ($^{\circ}\text{C}$), and T_r is a plate temperature ($^{\circ}\text{C}$) [28].

$$Q_{\text{rad}} = A_r \varepsilon_r \sigma (T_r^4 - T_{\text{am}}^4) \quad (19)$$

where ε_r is a receiver remittance, and σ is a Stefan-Boltzmann constant (5.67×10^{-8}) ($\text{W}/\text{m}^2 \cdot \text{K}^4$). Also, can calculate the absorbed heat rate that defines (Q_{abs}) by using the equation below [30]:

$$Q_{\text{abs}} = Q_u + Q_{\text{loss}} \quad (20)$$

where Q_u is the valuable heat gain (W).

2.5. Solar still effectiveness

For an ideal system, the effectiveness represents the gain on the cost or the output by input and these could be present by the following equation [28]:

$$\zeta_{\varepsilon} = \frac{Q_{\varepsilon}}{G_s} \times 100 \quad (21)$$

For the invented solar purified, the actual efficiency is given as [28]:

$$\zeta_{\varepsilon} = \frac{M_{\varepsilon}(I_{st} - I_w)}{G_{\varepsilon} \times 100} \quad (22)$$

From the overall heat balance equation on the still solar equation [29]:

$$Q_{\varepsilon} = \alpha_w T_g G_s - (q_c + q_b + q_r) \quad (23)$$

where α_w is an absorptivity of the water mass, T_g is the average temperature of the glass cover ($^{\circ}\text{C}$), G_s is average solar intensity/radiation (W/m^2), q_c is heat flux from the water surface to the cover by free convection (convective loss) transparent cover to ambient air (W/m^2), q_b heat loss through base and perimeter of base (W/m^2), and q_r is a amount of heat handover from the water surface to the shelter by radiation (W/m^2) [31].

$$q_c = h_c (T_w - T_g) \quad (24)$$

$$q_b = h_b (T_w - T_a) \quad (25)$$

$$q_r = F_s A_c \sigma (T_w^4 - T_g^4) \quad (26)$$

Moreover, the heat transfer by convection could be expressed as following [28]:

$$q_c = (7.734 \times 10^{-4}) \left[(T_w - T_g) + \frac{(P_w - P_g)(T_w + 273)}{2.65 P_T - P_w} \right]^{1/4} (T_w - T_g) \quad (27)$$

$$q_r = \frac{A\sigma(T_w + 273)^4 - (T_g + 273)^4}{\frac{1}{E_c} + \left[\frac{A_c}{A_g} \left(\frac{1}{E_g} - 1 \right) \right]} \quad (28)$$

Further the outer convection could be shown by the coefficient of convection as a function of wind speed [30,25]:

$$h_{cb} = 5.7 + 3.8v \quad (29)$$

Seeming v : is a wind velocity, m/s [22,28].

Moreover, the amount of sun still system generation could be expressed by following [31].

$$M_\varepsilon = \frac{Q_\varepsilon}{L} = \frac{G_\varepsilon \zeta}{(I_{st} - I_w)} \quad (30)$$

$$q_{ga} = \alpha_g G_s + q_c + q_\varepsilon + q_r \quad (31)$$

2.6. Cost analysis of the solar still

The project is based on calculating the (SFF) sinking fund factor (dimensionless), which represents the number of equal amounts to be paid at the end of a specified period of (n) is project life span at a periodic interest rate denoted (i) so that the payments accrue to a specific dollar amount at the end of that period. To calculate the SFF for 10 years at an annual interest rate of 4%, can be use the formula below [29]:

$$SFF = \frac{i}{(1+i)^n - 1} \quad (32)$$

The economic analysis of the project needs to calculate the CRF, which represents the capital recovery factor (dimensionless) through Eq (33) [30–32]:

$$CRF = SFF \times (1 + i)^n \quad (33)$$

One of the main pillars of calculating project costs is to find the FAC is the annual fixed cost (\$), which is represented by the following equation [29,31], where, P is the present capital cost (\$):

$$AFC = P \times CRF \quad (34)$$

It is necessary to calculate the salvage value (S) and the annual salvage value (ASV) to enhance the monetary value of the project, which represents the expected amount to sell the project at the end of ten years, measured in \$, as shown by the following equation [32,33]:

$$S = 0.2 \times P \quad (35)$$

$$ASV = SFF \times S \quad (36)$$

With the possibility of neglecting the value of AMC, which represents the cost of operating the annual maintenance because it does not exceed cleaning the device, however, it can be calculated from the following equation [34,35]:

$$AMC = 0.15 \times FAC \quad (37)$$

The economic feasibility of the project needs to calculate (AC) annual cost value with the cost of producing distilled water per liter(\$/L) CPL; and then compare it with the annual yield (liters) M, as shown in the following equations [35]:

$$AC = FAC + AMC - ASV \quad (38)$$

$$CPL = \frac{AC}{M} \quad (39)$$

Table 3 shows the economic feasibility of this device if it is compared with distilled water sold in the Iraqi markets (\$/liters, with profitability of more than 85% per year.

3. Design considerations

This section briefly describes various parameters vary together with the results got in the fabrication of the solar still. As shown in Figure 3 and Tables 2 to 4.

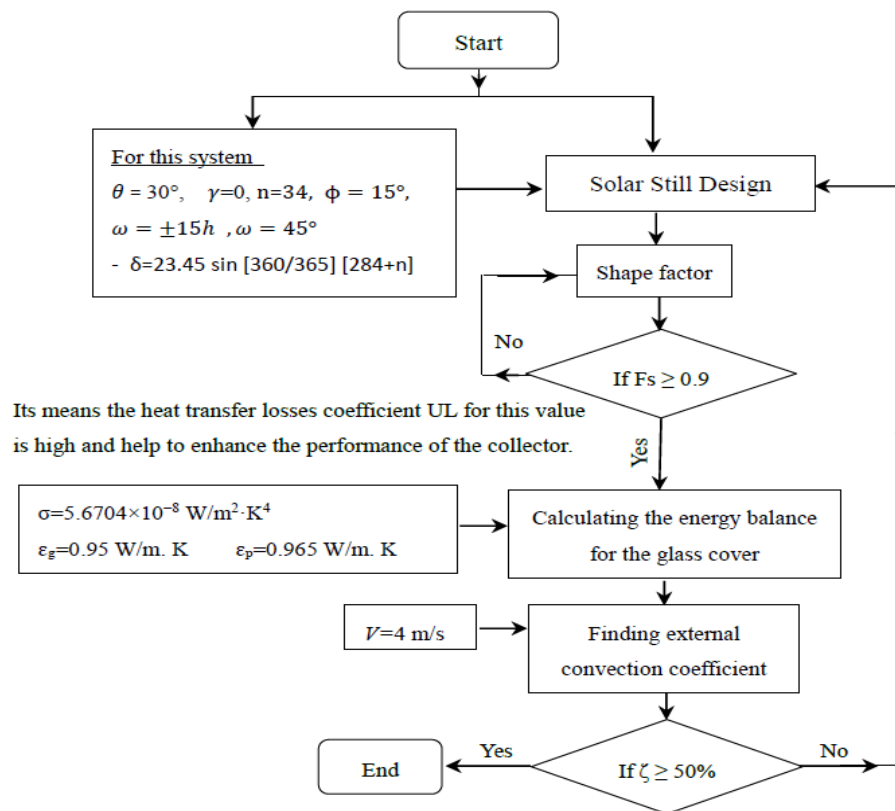


Figure 3. Flowchart for new solar still.

Table 2. Materials selection of component water purification system.

S/N	Component	Material(s)	Properties and comments
1	Collector/Glazing (Transparent)	Glass	<ul style="list-style-type: none"> • Low water absorptance. • Thickness (3 mm), and high. thermal conductivity • Translucent to short wave radiation. Transitivity = 0.9). • Low iron content. • Can withstand the effect. of weather, wind, sunshine, rain, dust, etc.
2	Basin (Absorber)	Glass with the base of Aluminum	<ul style="list-style-type: none"> • Thickness (4 mm). • High radiation absorptivity, and stable to corrosion. • High thermal conductivity.
3	Solar Reflector & Support Structure	Aluminum	<ul style="list-style-type: none"> • Minimum corrosion problem and cheaper. • High thermal conductivity. and high reflectivity.
4	Cover (Casing)	PVC	<ul style="list-style-type: none"> • Stable to corrosion with not poisonous. to water. • Inexpensive and readily available. and good insulator.
5	Insulator	corkboard	<ul style="list-style-type: none"> • Very cheap, Poor conductivity. and radiation of heat. • Very effective for insulation.
6	Sealant	Silicone Sealant	<ul style="list-style-type: none"> • Good resistance. to organic liquids. • Relax under high temperature. • Cheap and readily available.
7	Microcircuit	Arduino	<ul style="list-style-type: none"> • for calculating the amount. of moisture, heat and P.H. • Facilitating the use of interactive electronics in multidisciplinary projects
8	Black cloth pieces	Cotton	<ul style="list-style-type: none"> • Absorbs water slowly, which helps the water evaporate effectively. • Works to achieve the principle of evaporation of water from clothes.

Table 3. Heat balance and energy vector on the solar still.

S/N	Initial data	Calculation	Results
1	$T_w = 57\text{ }^\circ\text{C} = 330\text{ K}$ $T_g = 41\text{ }^\circ\text{C} = 314\text{ K}$ $\sigma = 5.6704 \times 10^{-8}\text{ W/m}^2\cdot\text{K}^4$ $\varepsilon_g = 0.95\text{ W/m. K}$ $\varepsilon_p = 0.965\text{ W/m. K}$	$F_s = \frac{1}{\frac{1}{\varepsilon_p} + \left[\left(\frac{A_c}{A_g} \right) \times \left(\frac{1}{\varepsilon_g} - 1 \right) \right]}$	Shape factor $F_s = 0.941$
2	Eq (26) Eq (29)	$q_r = F_s A_c \sigma (T_w^4 - T_g^4)$ $h_{cb} = 5.7 + 3.8v$	$q_r = 90.467\text{ W/m}^2$; $F_s = 0.941$
3	$V = 4\text{ m/s}$	$h_{cb} = 20.9\text{ W/m}^2 \times 2$ inclined transparent lid	External convection coefficient $h_{cb} = 41.8\text{ W/m}^2\cdot\text{K}$

Continued on next page

S/N	Initial data	Calculation	Results
	From Figure (5)		
	$U_b = \frac{1}{\frac{X_{ins}}{K_{ins}} + \frac{X_{cs}}{K_{cs}} + \frac{1}{h_{cb}}}$		
4	$h_{cb} = 41.8 \text{ W/m}^2 \cdot \text{K}$ $X_{cs} = 0.03 \text{ m}, X_{ins} = 0.04 \text{ m}$ $K_{cs} = 0.21 \text{ W/m}^2 \cdot \text{K}$ $K_{ins} = 0.038 \text{ W/m}^2 \cdot \text{K}$	$U_b = \frac{1}{\frac{X_{ins}}{K_{ins}} + \frac{X_{cs}}{K_{cs}} + \frac{1}{h_{cb}}}$	$U_b = 0.89 \text{ W/m}^2 \cdot \text{K}$
5	From equation 25	$q_b = U_b(T_w^4 - T_g^4)$	$q_b = 19.055 \text{ W/m}^2 \cdot \text{K}$
	From equation 22		The overall efficiency of the
6	$q_c = 66.8 \text{ W/m}^2,$ $Q_\varepsilon = 129.03 \text{ W}$	$\zeta_\varepsilon = \frac{Q_\varepsilon}{G_s} \times 100$	Solar Still = 78%

Table 4. Cost analysis for solar still, and the payments are at the end of 10 years.

SFF	FAC		S	ASV	AC		CPL		
Start with year (1)	End with year (10)	CRF	P = 200\$ @ Year (1)	From 1 to 10 years	Start with year (1)	End with year (10)	Start with year (1)	End with year (10)	M = 120 \$
1	0.0832	0.123	24.6 \$	4.92 \$	4.92 \$	0.41 \$	29.68 \$	34.19 \$	0.25 \$/L

3.1. Description of the proposed system

The proposed system consists of two main components including:

- 1- Collector: It consists of the following parts:
 - Supportive structure: it consists of light Aluminum and insulating plates painted.
- 2- Insulating base: It consists of insulating material, as shows in Figure 4.

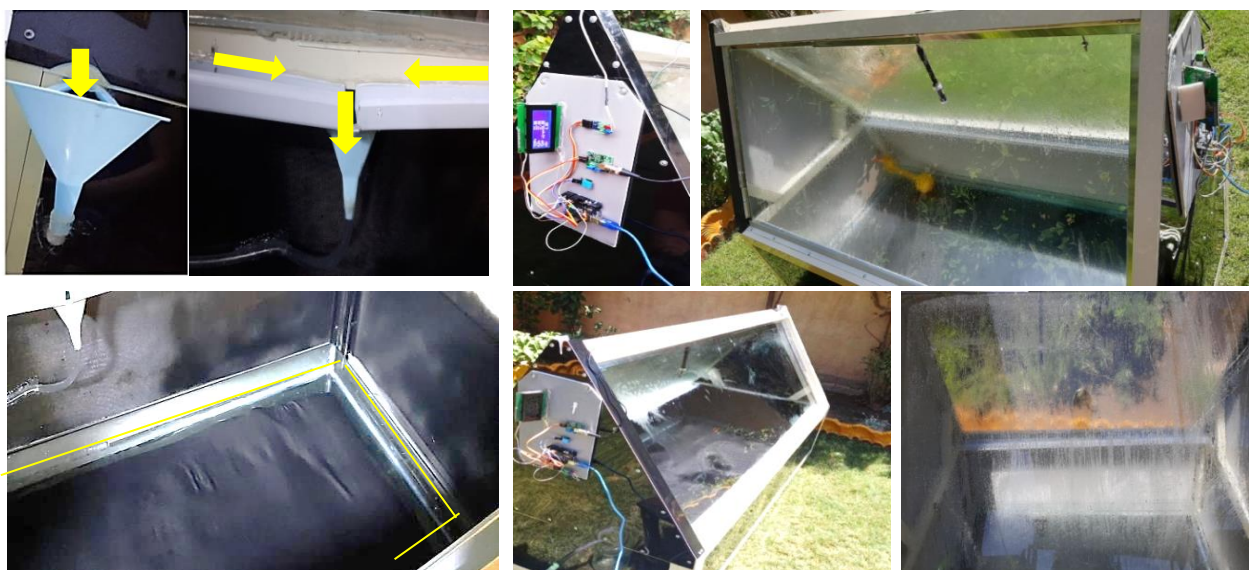


Figure 4. Solar still system.

3- Measurements unit: All measurement instruments are calibrated before starting the experiments and collecting data, and the instruments consist of the following:

- Digital temperature sensor.
- Arduino mega. LCD (20 × 40): Arduino type MEGA 2560 has used for data acquisition. Arduino is an open-source electronics platform that can read input and turn it into an output.
- Arduino card type Mega microcontroller board has (54) digital input/output pins, (15) analogue inputs, (16) UARTS, (4) hardware serial ports. A 16 MHz crystal oscillator, a USB connection, a power jack, an ICSP header, and a reset button, and show in Figure 5.

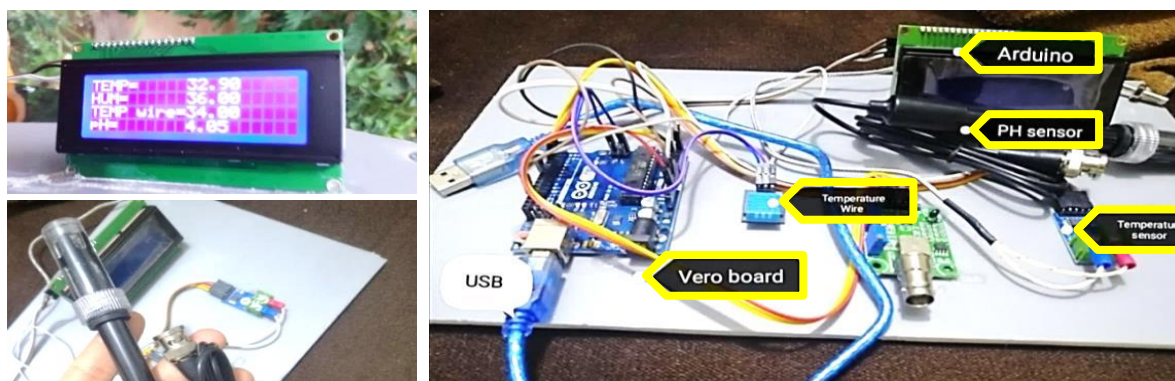


Figure 5. A board on which all measuring devices are installed.

4. Results and discussions

The experimental duration has been decided between the 1st of June to the 20th of July 2021, from 5:00 AM to 10:00 PM. Two scenarios assessed the influence of four factors: solar radiation, ambient temperature, water depth, and the daily output outputs for the solar still. The first used a 3 cm water level in the basin, and the second used a 0.75 cm water level with black cloth (1 × 0.75) cm in the basin. Water had collected from the Diyala River at the same depth in scenario one in the second scenario. The results include the following points:

4.1. Ambient temperature

The practical side showed that the humidity increases in the degree of condensation when the dew increases. The dew point is related to the relative humidity and the dry-bulb temperature. Therefore, the high relative humidity pushes the dew point closer to the dry air temperature. Relative humidity of 100% indicates that the dew point is equal to the temperature of dry air, and it's wholly saturated with water vapor. Figure 6 presents the results of the tests related to the relationship between the change in the ambient temperature during the days of the tests. We find a difference in temperature versus time significantly affecting the distillate. It increases when the temperature of the water and the glass decreases due to the difference in the ambient temperature.

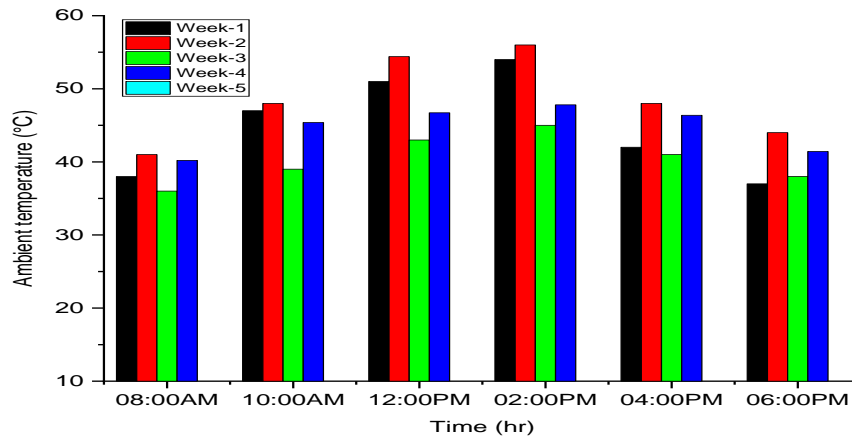


Figure 6. Ambient temperature at experimental period.

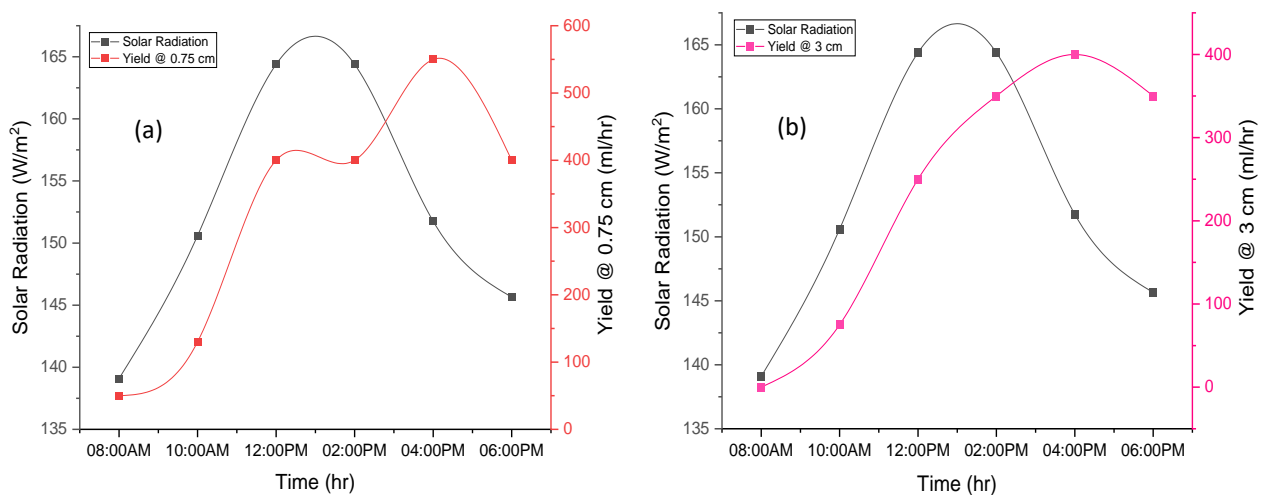


Figure 7. Relation between solar radiation and yield amount (a) 0.75 cm, and (b) 3 cm.

The productivity of fresh water is affected by the difference in the evaporation temperature in the surrounding conditions, not to mention the incoming solar radiation in the field of solar energy collection. Figure 7 shows the extent of water creation and solar radiation condition during the test period. The test results show the system's water manufacture with different water depths in the basin (0.75 and 3) cm. The output can reach 550 ml/h, with an average solar radiation intensity of 165 W/m² at a depth of 75 cm. But the freshwater yield was less than 400 ml/h at a depth of 3 cm, representing the best harvest during the experimental period. The difference in values is due to the difference in weather and the decrease in the intensity of solar radiation. These results indicate that the system production is closely related to the solar irradiance status.

Figure 8 represents the relationship between pond temperature and yield. Moreover, the results showed that less water poured into the base will ensure more water condensation, and this may be due to the energy saved to heat the dirty water and use it to vaporize it. The results of the five-week test show that the temperature of the aquarium balances with the difference in solar radiation, and the temperature of the aquarium can rise to about 70 °C when the solar radiation

reaches 165 W/m^2 . This affects the amount of relative humidity, which ranges between 60% and 80%.

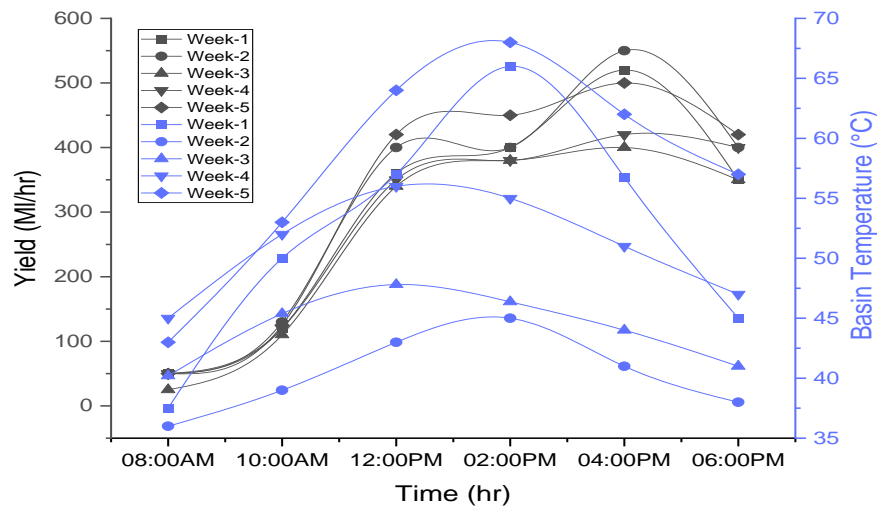


Figure 8. The relations between basin temperatures with yield amount.

4.2. Effect of salt on water production

Water amount in solar purified plays a vital role in the performance of the system. Experiments have conducted with two different water depths, 3 cm, 0.75 cm, in the solar still. The experimentation included two samples of water with various saline concentrations. The objective is to analyze the effects of saline concentrations on the yield of the distillate obtained. Two different salt concentrations have taken from available data at various sites. The first time takes a saltwater concentration of about 372 ppm from the house tap. Then, using this water in a solar still and a saline concentration has obtained, 78 ppm. The second time uses the Diyala River with a concentration of 537 ppm. With the same step, purified water has obtained with an estimated salinity of 85 ppm. Figure 9 demonstrates that attaining a higher yield with low salt concentration is due to solar energy absorption rate. The incidence of salt awareness and scaling in the basin will absorb some of the heat, and therefore there will be fewer heat available for water.



Figure 9. Observation of total dissolved salts yields from (a) house tap, (b)Diyala River.

Solar purification rate can be increased by supplying higher temperature water input. If the solar water heater is used with solar still, then yield can be increased. Out of the variables listed above and different parameters, the following parameters were selected for experimental analysis: effect of type of system, water depth, adding heat storage material, and effect of salt concentration.

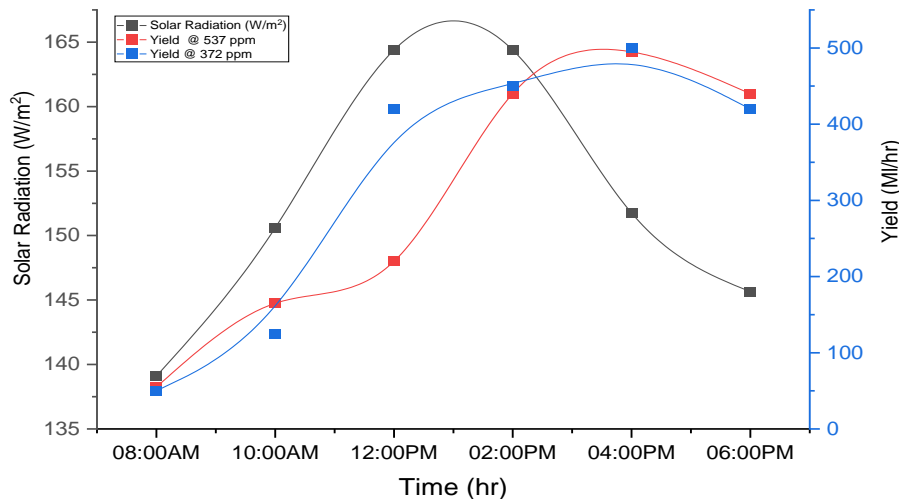


Figure 10. Relation between solar radiation and yield amount@ (372 & 537) ppm.

4.3. Effect of humidity on water production

Humidity depends on the temperature and pressure of the system. The relevant variable is the degree of saturation. The amount of water vapor needed to achieve saturation increases for increasing temperatures. As the temperature of a specific portion of the air decreases, it will eventually reach its saturation point without adding to or losing the mass of water. The amount of water vapor has contained within a given portion of the air can vary greatly. For example, a certain amount of near-saturated air contains 28 g (0.99oz) of water per cubic meter of air at 30 °C.

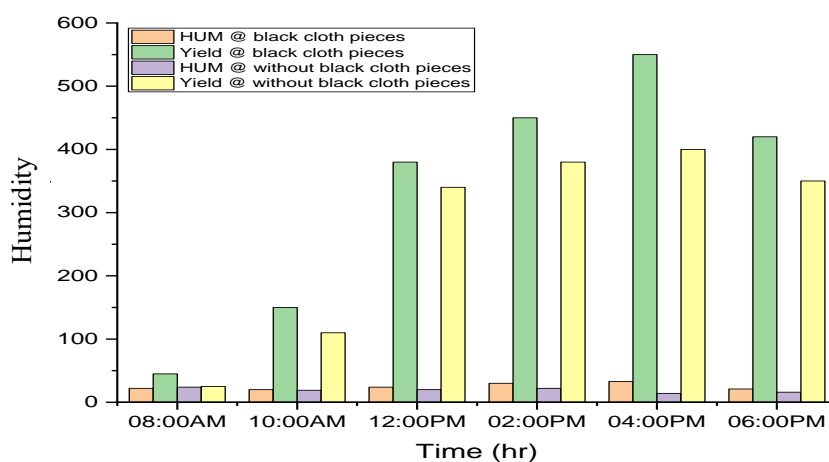


Figure 11. Effect of humidity on the amount of production by adopting the imposed scenarios.

However, it contains only 8 g (0.28 oz) water per cubic meter of air at 8 °C. This is defined as the humidity ratio for moist air (g/kgda). Figure 11 shows the effect of humidity on the amount of production during the study period.

4.4. Effect of black cloth pieces on water production

Figure 12 shows that the effectiveness of the second scenario in obtaining pure water at the same operating conditions at the outside temperature.

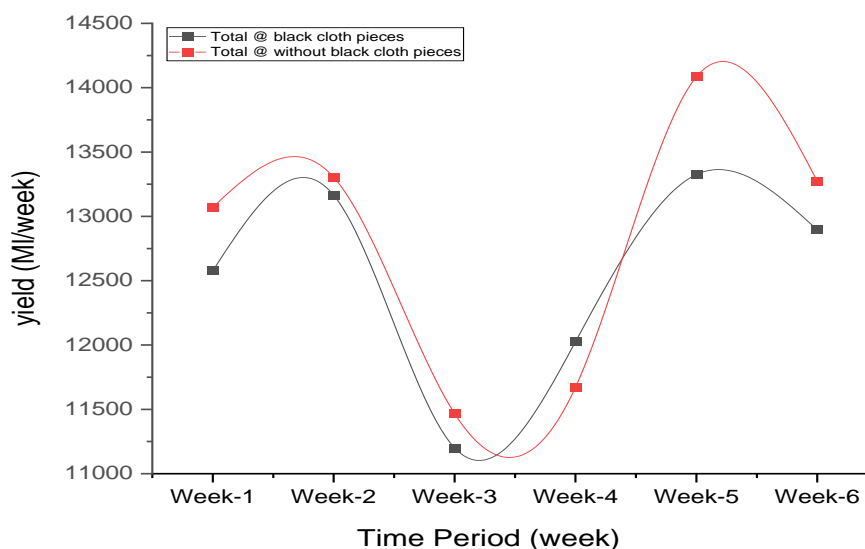


Figure 12. Observation of total yield for the second scenario under the same conditions.

The amount of moisture increases significantly in the presence of black cloth pieces. That helps to harvest more water if compared with the first scenario. Moreover, in the winter, the use of black cloth pieces ensures the evaporation of the water by increasing temperature better than other base colors.

4.5. Increasing condensation rate by using a wet pad for cooling the glaze surface

The direct cooling effect on the condensing surface is measured by wiping one side of the solar collector with a cloth dampened with water. This process repeats every hour to ensure the condensation of water shown in Figure 13.

Through these results, the cooling process has a clear and practical effect. The reason is due to the high temperatures in Iraq, unlike the European climate. That calls for the frequent adoption of this method, especially of this method frequently, especially in periods of the highest solar radiation. Appropriately, the rate of improvement in production amounted to about 170% compared to the conventional method. For example, at 2:00 pm, the condensation rate has increased from 300 ml/hr. to about 520 ml/hr. due to use the wet pad for cooling glass surface to stimulate the condensation process. The results have aligned with the theoretical predictions of the water condensation rate, which is about 400 to 600 ML/hr. depending on the type of water used, contamination level and salt concentration rate [29].

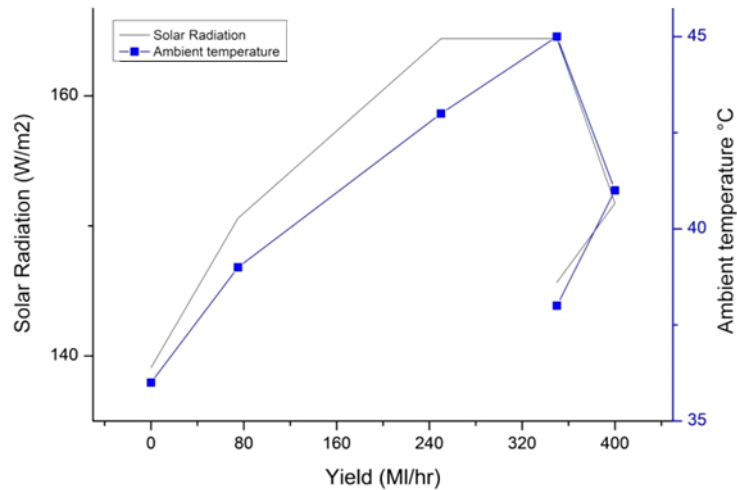


Figure 13. Mechanism of movement and work of the wet pad.

Figures 14 and 15 show the variation of freshwater condensation rate relative to the changing of ambient temperature and solar radiation rate.

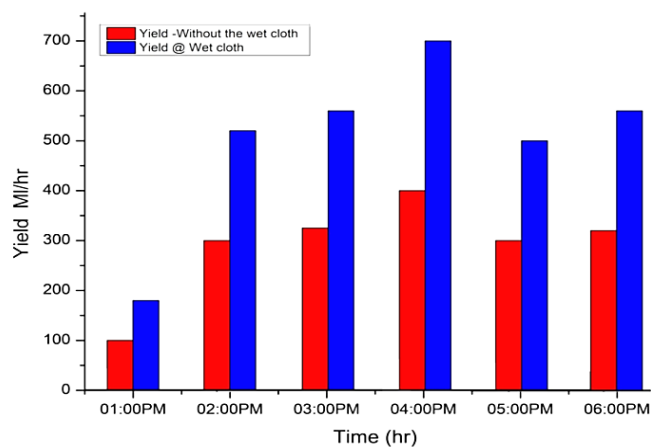


Figure 14. The difference in the amount of water produced if the wet cloth is used or not.

Furthermore, water production changing rate clearly points to the increasing for decreasing of ambient temperature throughout the day light (i.e., from sun rise to sun set).

The amount of water condensation rate is directly proportional to basin temperature and solar radiation rate as shown in Figure 16. For example, when temperature in the basin reaches about 60 °C but at the middle of the day yield rate is about 540 ml/hr. Moreover, the researchers may notice some time delay in the condensation rate relative to the temperature because the heating up takes a while for evaporating water and reaching to the upper surface for condensation. Therefore, the best way to evaluate condensation rate is by calculating the average yielding ml/hr. as average during the test day. Finally, the average pure water is harvesting from this distillation system for each square meter was about 0.282 L/day.

Meal No.	Time
1	1:00
2	1:02
3	1:03

1. The wiping begins at the beginning of the hour (for the first meal) from the top of the glass face.
2. After a minute, the wet joint is moved to the (second area) and continues for a minute for the third area.
3. The steps are repeated for the rest of the time.

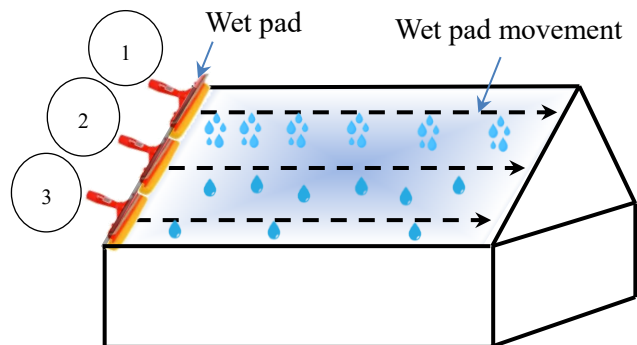


Figure 15. Mechanism of movement and work of the wet pad.

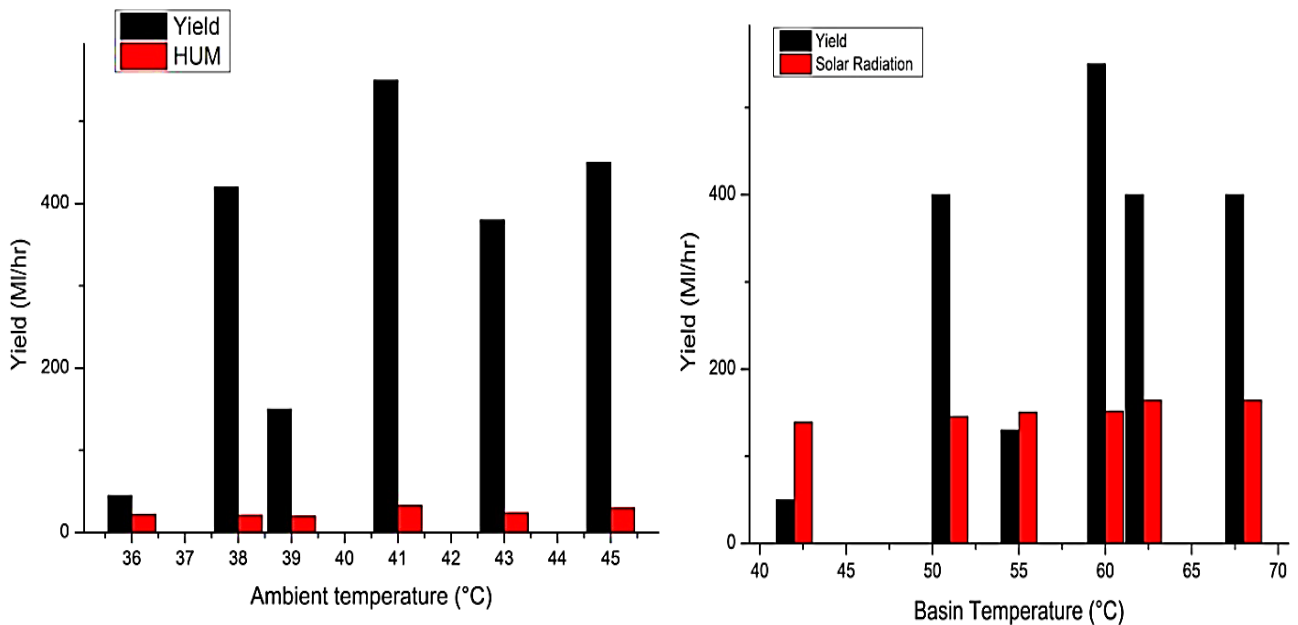


Figure 16. Impact of (a) ambient temperature on the water condensation rate (b) basin temperature on the water yield rate.

5. Conclusions

This study represents an essential contribution to understanding the stilled system, especially in a hot and dry climate. The wet pad design for cooling the outside glass surface, which is not in the direction of solar incidence, impacts the water condensation rate significantly. The reason for this increase in water is the decreasing surface temperature. Cooling the surface will increase the chance of condensation based on the principle of HVAC for moist air properties in regards to the dew point temperature.

In addition, the results show that this design can harvest 2 L/day of pure water by adding 5 liters of saline water, improving water purity by 209%.

Two scenarios have been set for the experiment. This study proves the behavior of solar systems experimentally in climates such as Iraq. The condition may be applied to several other several other golf countries in the Middle East.

Finally, this method of using water may represent one of the crucial approaches for sustainable architecture.

Acknowledgement

The researchers extend thanks and appreciation to the University of Diyala, College of Engineering, for completing this research and producing it as required.

Conflict of interest

The authors declare no conflict of interest.

References

1. Abahussain AA, Abdu ASh, Al-Zubari WK, et al. (2002) Desertification in the Arab Region: analysis of current status and trends. *J Arid Environ* 51: 521–545. [https://doi.org/10.1016/S0140-1963\(02\)90975-4](https://doi.org/10.1016/S0140-1963(02)90975-4)
2. Worthington AC, Hoffman M (2008) An empirical survey of residential water demand modelling. *J Econ Surv* 22: 842–871. <https://doi.org/10.1111/j.1467-6419.2008.00551.x>
3. Amiri A, Brewer CE (2020) Biomass as a renewable energy source for water desalination: a review. *Desalin Water Treat* 181: 113–22. <https://doi.org/10.5004/dwt.2020.25130>
4. Seckler D, Upali A (2000) Water supply and demand, 1995 to 2025. IWMI, *Annu Rep* 1999–2000: 9–17. Available from: <http://www.iwmi.cgiar.org> (accessed July 10, 2022).
5. Mahler ED, Zervas PL, Sarimveis H, et al. (2010) Determination of the optical tilt angle and orientation for solar photovoltaic arrays. *Renewable Energy* 35: 2468–2475. <https://doi.org/10.1016/j.renene.2010.03.006>
6. Eltawil MA, Zhao Z, Yuan LQ (2009) A review of renewable energy technologies integrated with desalination systems. *Renewable Sustainable Energy Rev* 13: 2245–2262. <https://doi.org/10.1016/j.rser.2009.06.011>
7. Alkaisi A, Mossad R, Sharifian-Barforoush A (2017) A review of the water desalination systems integrated with renewable energy. *Energy Procedia* 110: 268–274. <https://doi.org/10.1016/j.egypro.2017.03.138>
8. Kashyout AB, Hassan A, Hassan G, et al. (2021) Hybrid renewable energy/hybrid desalination potentials for remote areas: Selected cases studied in Egypt. *RSC Adv* 11: 13201–13219. <https://doi.org/10.1039/D1RA00989C>
9. Agrawal A, Rana RS (2019) Theoretical and experimental performance evaluation of single-slope single-basin solar still with multiple V-shaped floating wicks. *Heliyon* 5: e01525. <https://doi.org/10.1016/j.heliyon.2019.e01525>

10. Srivastava PK, Agrawal SK (2013) Experimental and theoretical analysis of single sloped basin type solar still consisting of multiple low thermal inertia floating porous absorbers. *Desalination* 311: 198–205. <https://doi.org/10.1016/j.desal.2012.11.035>
11. Abdel-Rehim ZS, Lasheen A (2007) Experimental and theoretical study of a solar desalination system located in Cairo, Egypt. *Desalination* 217: 52–64. <https://doi.org/10.1016/j.desal.2007.01.012>
12. Yuan GF, Wang ZF, Li HY, et al. (2011) Experimental study of a solar desalination system based on humidification–dehumidification process. *Desalination* 277: 92–98. <https://doi.org/10.1016/j.desal.2011.04.002>
13. El-Bialy E, Shalaby SM, Kabeel AE, et al. (2016) Cost analysis for several solar desalination systems. *Desalination* 384: 12–30. <https://doi.org/10.1016/j.desal.2016.01.028>
14. Abuelnuor AAA, Omara AAM, Musa HMH, et al. (2020) Experimental study on solar still desalination system integrated with solar collector and phase change material. *International Conference on Computer, Control, Electrical, and Electronics Engineering (ICCCEEE)*. <https://doi.org/10.1109/ICCCEEE49695.2021.9429589>
15. Aburideh H, Deliou A, Abbad B, et al. (2012) An experimental study of a solar still: Application on the sea water desalination of Fouka. *Procedia Eng* 33: 475–484. <https://doi.org/10.1016/j.proeng.2012.01.1227>
16. Choong WS, Zhi YH, Bahar R (2020) Solar desalination using fresnel lens as concentrated solar power device: An experimental study in tropical climate. *Front Energy Res*: 257–260. <https://doi.org/10.3389/fenrg.2020.565542>
17. Nafey AS, Abdelkader M, Abdelmotalip A, et al. (2001) Solar still productivity enhancement. *Energy Conversion Manage* 42: 1401–1408. [https://doi.org/10.1016/S0196-8904\(00\)00107-2](https://doi.org/10.1016/S0196-8904(00)00107-2)
18. Jamil B, Akhtar N (2017) Effect of specific height on the performance of a single slope solar still: An experimental study. *Desalination* 414: 73–88. <https://doi.org/10.1016/j.desal.2017.03.036>
19. Omara ZM, Hamed MH, Kabeel AE (2011) Performance of finned and corrugated absorbers solar stills under Egyptian conditions. *Desalination* 277: 281–287. <https://doi.org/10.1016/j.desal.2011.04.042>
20. Tripathi R, Tiwari GN (2006) Thermal modeling of passive and active solar stills for different depths of water by using the concept of solar fraction. *Sol Energy* 80: 956–967. <https://doi.org/10.1016/j.solener.2005.08.002>
21. AlKtraneea MHR, Al-Yasiric Q, Kabeel AE (2020) Improving the productivity of a single-slope solar still using Fresnel lenses under Iraq climatic conditions. *Desalin Water Treat* 205: 22–30. <https://doi.org/10.5004/dwt.2020.26424>
22. Panchal H (2016) Performance investigation on variations of glass cover thickness on solar still: experimental and theoretical analysis. *Technol Econ Smart Grids Sustainable Energy* 1: 1–11. Available from: <https://link.springer.com/article/10.1007/s40866-016-0007-0>.
23. Kumar PN, Manokar AM, Madhu B, et al. (2017) Experimental investigation on the effect of water mass in triangular pyramid solar still integrated to inclined solar still. *Groundwater Sustainable Dev* 5: 229–234. <https://doi.org/10.1016/j.gsd.2017.08.003>

24. Ahmed AM, Ahmed AH, Daoud RW, et al. (2020) Optimization of simple solar still performance using fuzzy logic control. *2020 6th International Engineering Conference "Sustainable Technology and Development"(IEC), IEEE*, 1112–1124. <https://doi.org/10.1109/IEC49899.2020.9122819>
25. Al-Musawi OAH, Khadom AA, Ahmadun FB, et al. (2018) Water distillation in a combined solar still and solar pond system: Iraq as a case study. *Euro-Mediterranean J Environ Integ* 3: 1–14. <https://doi.org/10.1007/s41207-018-0057-x>
26. Siraki AG, Pillay P (2012) Study of optimum tilts angles for solar panels in different latitudes for urban applications. *Sol Energy* 86: 1920–1928. <https://doi.org/10.1016/j.solener.2012.02.030>
27. Al-Samari A, Almahdawi YAJ, Al-Rubaye LAH (2020) Design of absorption refrigeration system using solar energy resource. *Int J Air-Cond Refrig* 28: 2050025. <https://doi.org/10.1142/S201013252050025X>
28. Robert F, Majid G, Alma C (2010) Renewable energy and the environment. *CRC Press, Taylor Francis Group*. Boca Raton: 7–49. Available from: https://cds.cern.ch/record/1611523/files/9781420075663_TOC.pdf.
29. Jabbar MFA, Al-Ma'amar AF, Shehab AT (2010) Change detections in marsh areas, south Iraq, using remote sensing and GIS applications. *Iraqi Bull Geol Min* 6: 17–19. Available from: <https://www.iasj.net/iasj/download/666b43dc81ae4b45>.
30. Stapleton G, Neill S (2012) Grid-connected solar electric systems. *Taylor Francis Group, (LLC)*. <https://doi.org/10.4324/9780203588628>
31. Kumar S, Tiwari GN (2009) Life cycle cost analysis of single slope hybrid (PV/T) active solar still. *Appl Energy* 86: 1995–2004. <https://doi.org/10.1016/j.apenergy.2009.03.005>
32. Al-Sudani HIZ (2019) Rainfall returns periods in Iraq. *J Univ Babylon Eng Sci* 27: 1–9. <https://doi.org/10.29196/jubes.v27i2.2288>
33. Al-Samari A, Almahdawi AR (2020) Design of absorption refrigeration system using solar energy resource. *Int J Air-Cond Refrig* 28: 205–212. <https://doi.org/10.1142/S201013252050025X>
34. Kazema HA, Albadib MH, Al-Waelic AHA, et al. (2017) Techno-economic feasibility analysis of 1 MW photovoltaic grid connected system in Oman. *Case Stud Therm Eng* 1: 131–141. <https://doi.org/10.1016/j.csite.2017.05.008>
35. Azevedo FDASM (2014) Renewable energy powered desalination systems. Available from: <http://hdl.handle.net/10451/15792>.



AIMS Press

© 2022 the Author(s), licensee AIMS Press. This is an open access article distributed under the terms of the Creative Commons Attribution License (<http://creativecommons.org/licenses/by/4.0>)